

# Processing of Nano-Y–TZP/ $\text{Al}_2\text{O}_3$ Composites. II: Compaction and Sintering Behaviour of Nano-Y–TZP/ $\text{Al}_2\text{O}_3$ Composite Powders

J. L. Shi, J. H. Gao, B. S. Li & T. S. Yen

Shanghai Institute of Ceramics, Chinese Academy of Sciences, 1295 Ding-Xi Road, Shanghai, 200050, P.R. China

(Received 31 August 1994; revised version received 9 March 1995; accepted 20 March 1995)

## Abstract

*The compaction and sintering behaviour of nano-sized and well-dispersed Y–TZP/ $\text{Al}_2\text{O}_3$  composite powders have been investigated. It has been found that the composite powders contained no hard agglomerates, and after compaction, all soft agglomerates are fragmented. The green density of the compact was found to decrease with the increase of alumina content. The composite powder compacts containing less than 20 mol% alumina can be sintered at not higher than 1350°C to 99% of their theoretical densities. The densification behaviour of the composite powders show duplex shrinkage peak characteristics for the composites containing not less than 15 mol% alumina.*

## 1 Introduction

Reports have shown that zirconia (or Y–TZP)/alumina composites exhibit higher performance than single phase alumina or TZP ceramics.<sup>1–7</sup> For the alumina matrix based composite ceramics, the main toughening and strengthening mechanisms are zirconia phase transformation and microcracking.<sup>1–4</sup> Another kind of composite is TZP, (mainly Y–TZP) based composite; this kind of composite also shows higher toughness and strength than single TZP ceramics. The toughening effect of the composite has been found to be increased phase transformation volume of Y–TZP by the addition of alumina particles in the Y–TZP matrix.<sup>9</sup>

As stated in the previous paper, the composites were more difficult to densify than the single matrix phase.<sup>9–11</sup> So depending on the powder properties, hot-pressing or hot-isostatic pressing techniques may be required<sup>5–7</sup> for the full densification. This is because the second phase usually acts as an impedance to the densification if the particles of the second phase were too large com-

pared to the matrix phase, or if the composite powders were possibly strongly agglomerated. Pressureless sintering may also be useful if the particles of the second phase are not much larger than that of the matrix,<sup>12</sup> but the sintering temperature must be higher than the matrix because of the duplex pore size distribution led by the larger second phase.<sup>13</sup> Providing that the hard-agglomerate-free composite powders with roughly the same particle sizes between the second and matrix phases can be prepared, they could have good sinterability comparable to the matrix. In the previous paper, such a composite powder has been successfully prepared<sup>14</sup> and the sintering behaviour will be studied in this paper.

## 2 Experimental Procedure

The preparation process of the composite powders has been reported in the previous paper.<sup>14</sup> The powders were afterwards compacted first by uniaxial pressing at 50 MPa and followed by cold isostatic pressing at 250 MPa. The green densities of the composite powder compacts were calculated by their weights and the geometric volumes measured, and the theoretical densities were calculated according to the volume percentages of the composites. The compacts were also characterized by their pore size distributions to find if the agglomerates, (i.e. inter-agglomerate pores) were present in the compacts.

The shrinkage behaviour was recorded by a constant heating rate of 5°C/min on a linear dilatometer to 1550°C. Isothermal sintering was also conducted in a molybdenum silicide furnace at various temperatures for 120 min.

The sintered bodies were observed of their microstructure with scanning electron microscope (SEM, JCSA-733, JEOL) and transmission electron microscope (TEM, JEM-200CX, JEOL).

### 3 Results

#### 3.1 The compaction behaviour

The agglomeration behaviour of the powders can be characterized by the pore size distributions of their compacts.<sup>11–12</sup> For agglomerate-free powder compacts, there are only one kind of pores—interprimary particle pores could be detected in the compacts. Fig. 1 shows the pore size distribution of the compacts of the composite powders calcined at 750°C. There was only one distribution peak detected in every kind of powder compact and therefore, there was only one kind of pore present in the compacts, which were the interprimary particle pores, meaning that no agglomerates were present in the compacts. Figure 2 gives the mean pore sizes and the size ratios of the pores to the grains as a function of alumina content. The pore size decreased with the increase of alumina

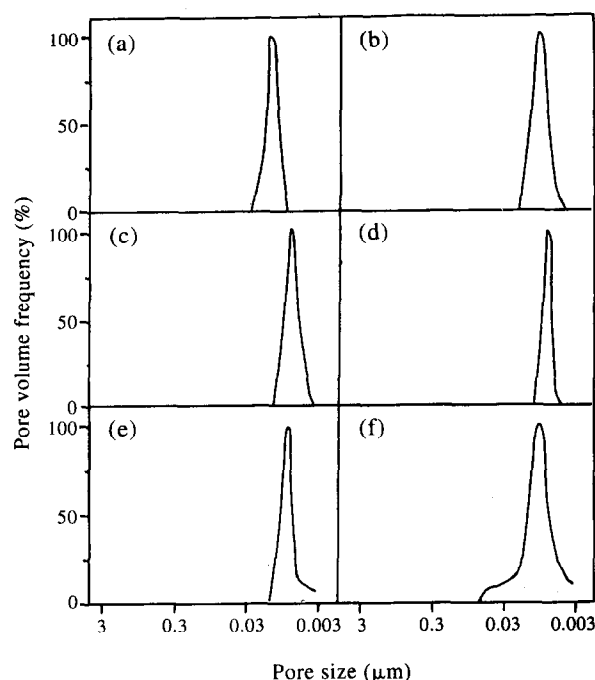


Fig. 1. Pore size distributions of the 750°C calcined composite powder compacts (250 MPa) containing (a) 0, (b) 10, (c) 15, (d) 20, (e) 30, (f) 45 mol% alumina.

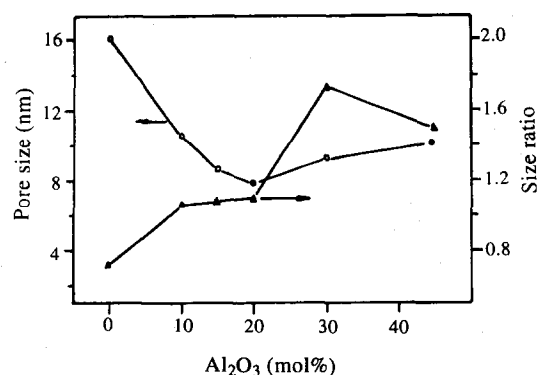


Fig. 2. Dependence of the pore size and the size ratio of pores to particles on the alumina content in the composite powder compacts (750°C calcined, 250 MPa compacted).

content when the alumina content was less than 20 mol%, corresponding to the reducing effect of alumina on the crystallite size of Y-TZP,<sup>14</sup> however it increased slightly when above 20 mol%. The size ratio of the pores to the crystallites increased with the addition of alumina at not higher than 30 mol%, meaning the compaction properties of the primary particles of the composite powders have changed, as proved by the measurement of the green densities of the compacts (Fig. 3).

#### 3.2 Densification with constant heating rate

The densification behaviour of the composite powder compacts with constant heating rate measured is shown in Fig. 4. The figure shows that the

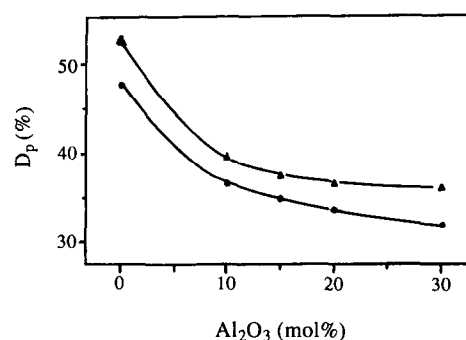


Fig. 3. Green densities of the composite powder compacts as a function of alumina content, (●) 750°C, (▲) 950°C.

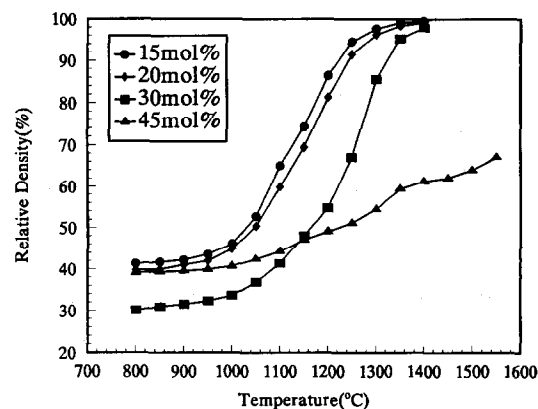
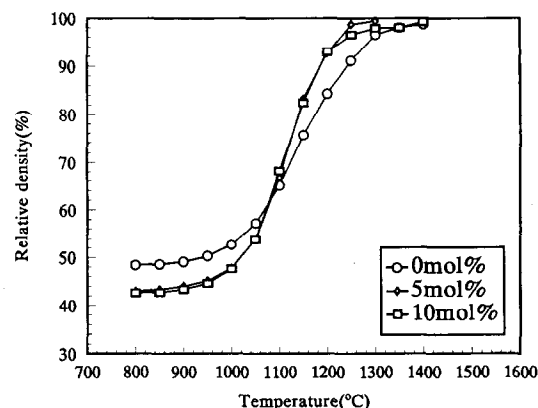


Fig. 4. Relative densities ( $\rho$ ) versus temperature profile of the composite powder compacts during sintering by a constant heating rate of 5°C/min at different alumina contents.

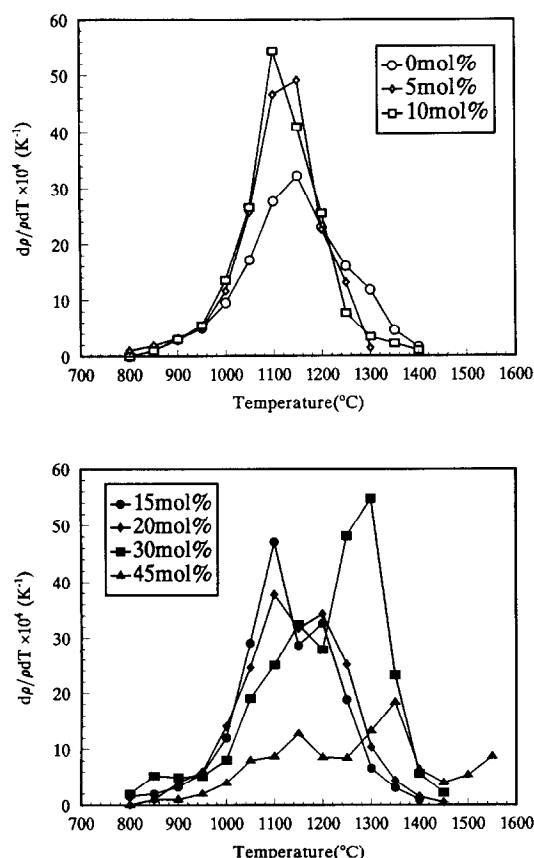


Fig. 5. Densification rate ( $dp/dT$ ) versus temperature profile of the composite powder compacts during sintering by a constant heating rate of  $5^\circ\text{C}/\text{min}$  at different alumina contents.

addition of 5–10 mol% alumina lowered the densification temperature from about  $1350^\circ\text{C}$  to about  $1250$ – $1300^\circ\text{C}$ , but the densification process finished at higher temperatures when the composite powders contained a higher percentage of alumina. For the composite powders containing 45 mol% alumina, full densification could not be reached.

Figure 5 gives the densification rates of the composite powder compacts. The densification rates were greatly raised by the addition of 5 or 10 mol% alumina in the composites, and temperatures for the end-point of densification were lowered. Much more interestingly, when the composites contained 15 or higher mol% of alumina, there were two maximum points of the densification rates, (duplex shrinkage peaks), during heating: one at about  $1050$ – $1100^\circ\text{C}$  and another at around  $1200^\circ\text{C}$  or higher. Despite this phenomenon, the composite powders could still be densified at about  $1400$ – $1450^\circ\text{C}$ , but if the alumina content was any higher, (45 mol%), there was only a small densification effect.

### 3.3 Densification with isothermal sintering

Figure 6 shows the sintering densities of the composite powder compacts at different temperatures. The results show again that nearly full densifica-

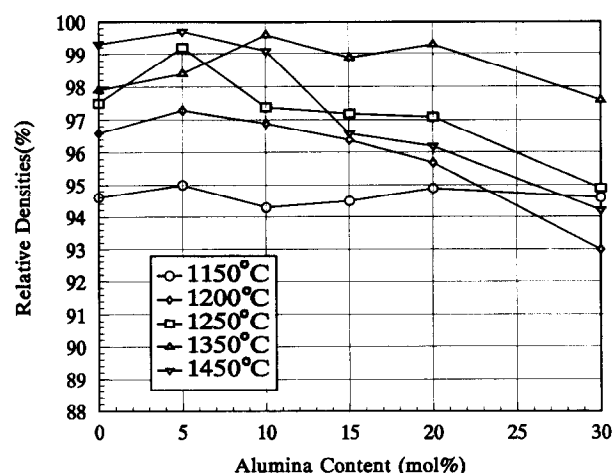


Fig. 6. Sintering densities of the composites at different sintering temperatures by isothermal sintering for 120 min.

tion could be obtained for the composites containing 5–20 mol% alumina at sintering temperatures as low as  $1250$ – $1350^\circ\text{C}$ ; the sintered densities were roughly the same as or even higher than those of single phase Y-TZP in the temperature range of  $1150$ – $1350^\circ\text{C}$  except for the composite containing 30 mol% alumina. At  $1450^\circ\text{C}$ , the sintering densities decreased for the composites containing 15 mol% or a high content of alumina.

### 3.4 Microstructure development

The presence of alumina does not only decrease the crystallite size in the coprecipitated composite powder, it also inhibits the grain growth in the composites, as shown in Fig. 7 and 8. The micrographs in Fig. 7 were obtained on the polished and thermally etched surface of the sample sintered at lower temperatures and no apparent contrast difference between the components could be distinguished in the micrographs. Those in Fig. 8 were the natural surfaces of the composite sintered at higher temperatures, and the contrasts between the particles can be clearly seen: the dark grains were alumina and others were Y-TZP. It is obvious from the micrographs that the microstructure is fine and homogeneous, and the grain size of the two phases of alumina and Y-TZP are almost the same.

Figure 9 shows the microstructure of a Y-TZP/45 mol% alumina composite sintered at  $1350^\circ\text{C}$ . The composite was not densified and the microstructure was highly porous.

Figure 10 shows the TEM microstructure of Y-TZP/20 mol% alumina composite sintered isothermally at different temperatures. In contrast to the micrographs shown in Fig. 8, in TEM micrographs, the dark grains are Y-TZP, the bright ones alumina. The grains of both Y-TZP and alumina grew with increasing sintering temperature.

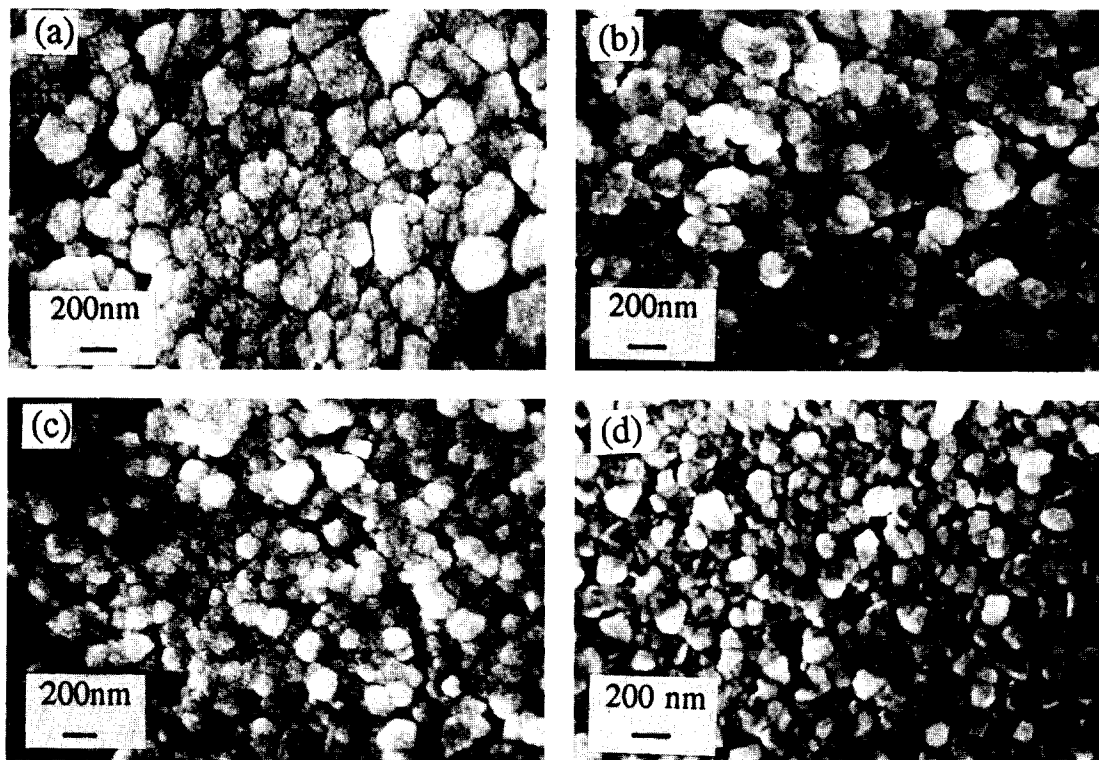


Fig. 7. Microstructure of the composites sintered at 1250°C for 120 min with alumina content of (a) 0, (b) 10, (c) 20 and (d) 30 mol%.

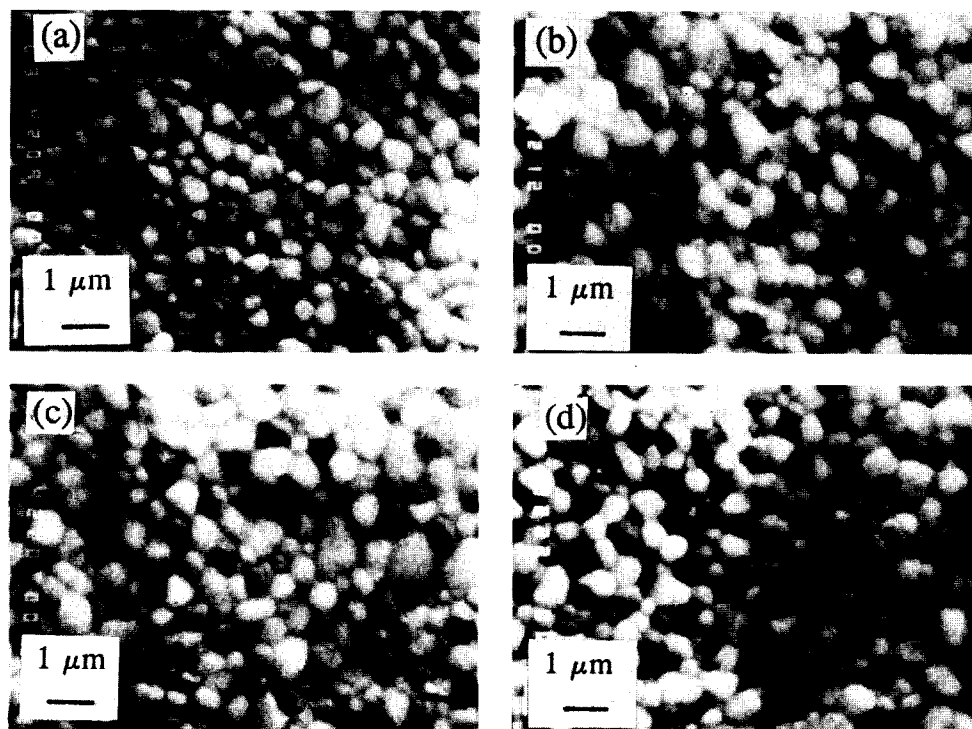


Fig. 8. Microstructure of the composites sintered at 1550°C for 120 min with alumina content of (a) 0, (b) 10, (c) 20 and (d) 30 mol%.

#### 4. Discussion

##### 4.1 Particle arrangement in the compact

Although the composite powders prepared are hard agglomerate-free and could be compacted with only one kind of pores — inter-primary particle pores left in the compacts — the packing properties between the primary particles were dependent on the alumina content. The size ratios

of the pores to primary particles increase with the increase of alumina content, corresponding to the decrease of the compaction densities. This phenomenon, if the agglomeration properties were not affected by the alumina addition, could be mainly attributed to the decrease of particle size when alumina was added. The dependence of the packing densities on the particle size is well known to ceramists, the poor flowability of fine powders

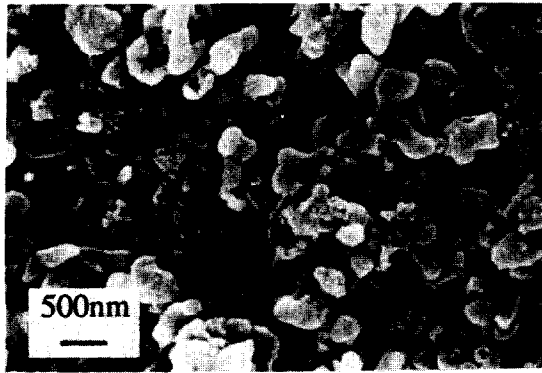


Fig. 9. Microstructure of Y-TZP/45 mol% alumina sintered at 1350°C for 120 min.

is the reason for their low packing densities. The dependence of compaction densities can be explained in a similar way. With the decrease of particle size, the contact between the particles in the unit area increases. Because of the non-deformability of the ceramic particles, the contact area for every contact is independent of particle size, so under a certain external pressure, the more contact between the particles causes lower effective internal pressure, which is the driving force for the rearrangement between particles. Thus, the compaction density would decrease with the decrease

ing of particle size. Higher applied pressure is needed for powders of finer particle sizes for the same density than that for powders of larger particle sizes.

#### 4.2 Densification characteristics as influenced by alumina

The great increase of the densification rate of the composite powders at 5 and 10 mol% alumina is not fully understood. Probably it is due to the smaller grain size of the composites than the single phase Y-TZP in the compacts during sintering.

Generally there is only one maximum value of the densification rate during sintering, with a constant heating rate of homogeneous powder compacts. This is true for the composites with not higher than 10 mol% alumina, the maximum temperature for this is around 1100°C. The occurrence of the second maximum value occurs at around 1200°C or higher (in addition to the first maximum value), for the composite powder compacts with higher alumina content can be understood by the phase transformation of alumina in the composite powder during sintering. As this process did not take place at a calcination temperature as low as 750°C but at around 1100–1200°C.<sup>14</sup> When the first maximum value was reached, the crystallization of

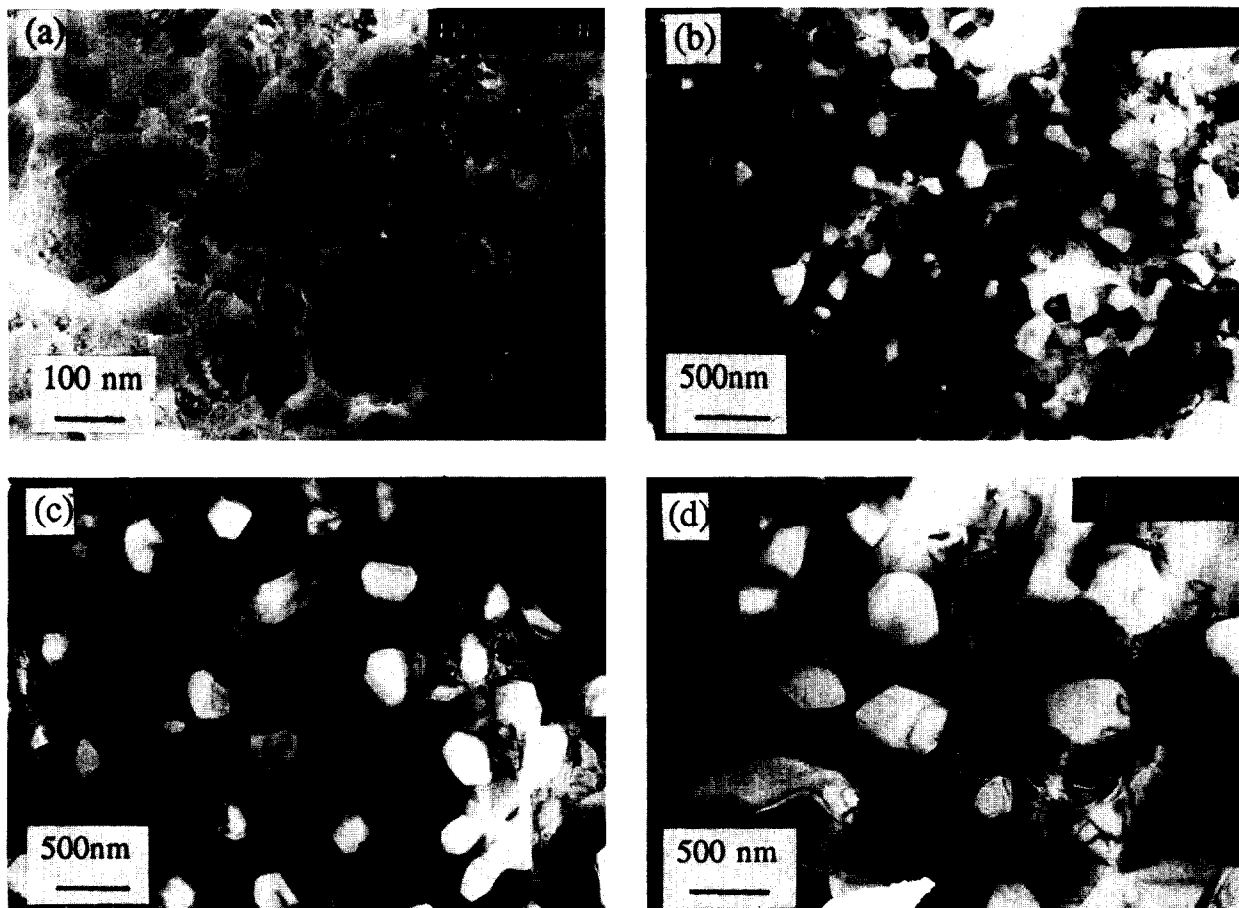


Fig. 10. TEM microstructure of the composites containing 20 mol% alumina sintered at (a) 1250, (b) 1350, (c) 1450 and (d) 1550°C for 120 min.

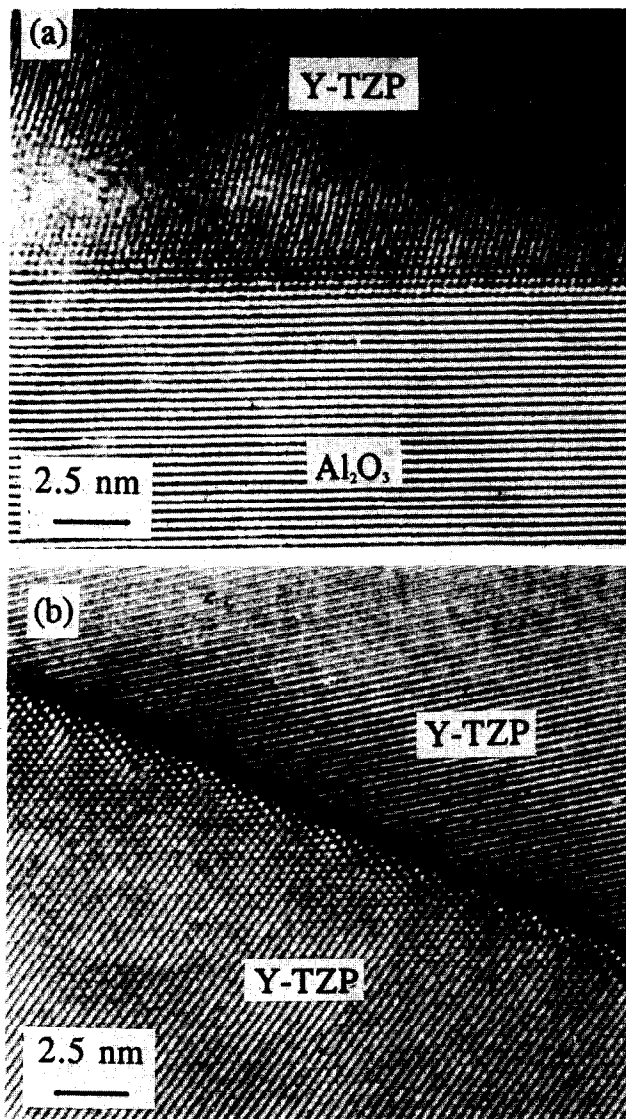


Fig. 11. Lattice images of the Y-TZP/20 mol% alumina composites sintered at 1450°C for 120 min for (a)  $\text{Al}_2\text{O}_3$ /Y-TZP interface, (b) Y-TZP/Y-TZP interface.

$\alpha$ -alumina from the Y-TZP matrix during sintering impeded the densification process of the composite and densification rate was lowered through the formation of the inter alumina Y-TZP pores, and/or the 'vermicular' structure between alumina particles, inhibiting matrix diffusion. As the temperature increased, the densification rate reached another maximum value through the enhancement of the diffusion ability at elevated temperatures. An alternative explanation for the second maximum densification rate may be that as the alumina content reaches 15 mol% or higher, the contacts between alumina particles increase and the alumina clusters may form, and the densification of the alumina cluster, together with the not necessarily retarded densification of Y-TZP, causes the second maximum rate. The temperatures for the second maximum were dependent on alumina content, and more alumina that is added, then

the impedance effect by alumina is larger and the second maximum densification rate occurs at higher temperatures.

The composite powder compacts could be densified to near full density when alumina content is not higher than 20 mol%. 30 mol% alumina in the composite has already prevented the composite from reaching full densification; at 45 mol% of alumina, the composite compact showed only very limited densification effect, partially because of the low green density, but mainly because higher alumina content, which forms an extensive 'vermicular' structure or even a network in the body. This vermicular network leads to a large amount of inter-alumina or inter-alumina-Y-TZP pores and densification becomes greatly impeded.

#### 4.3 The role of alumina in the development of the microstructure

The crystallization of alumina from Y-TZP grains during sintering leads to a two phase structure: alumina particles become homogeneously distributed in the Y-TZP matrix. Different from the similar composed but differently processed composites,<sup>9-13</sup> the particle size of the second alumina phase in this study was almost the same for those with the Y-TZP matrix (so no alumina particles could be trapped in a matrix grain or vice-versa), so the microstructure inhomogeneity was greatly suppressed. The particle size of the Y-TZP matrix was considerably affected by the presence of alumina particles at 1250°C: the matrix grain growth was inhibited by alumina. Figure 10 is the lattice image of a composite containing 20 mol% alumina. It can be seen that the interface between the two phases is very clear and no glass phase can be detected, so the inhibiting effect of grain growth by alumina is mainly from the pinning effect of the *in situ* formed second alumina phase. At a higher sintering temperature of 1550°C, the effect of grain growth inhibition of Y-TZP by alumina was not so strong as that at 1250°C.

#### 5 Conclusions

- (1) The composite powders prepared are hard, agglomerate-free and can be compacted without agglomerates left in the compacts.
- (2) The composites can be densified to full densities at relatively low temperatures of 1250–1350°C for 2 h when alumina content is not higher than 20 mol%.
- (3) The densification rate of the composite compacts with alumina content of 5 and 10 mol% is greatly increased because of the inhibited grain growth of the Y-TZP matrix.

Two maximum values of the densification rate (duplex shrinkage peaks) occur when alumina content is equal to or larger than 15 mol%, which is attributed to the phase transformation of alumina and/or the alumina particle clusters formed in the compacts during sintering.

- (4) The homogeneous microstructure of the composite was obtained with the same grain size of the matrix Y-TZP and the second phase of alumina. The inhibiting effect of alumina on the grain growth of Y-TZP is probably led by the pinning effect.

## References

1. Heuer, A. H., Claussen, N., Krive, W. M. & Ruehle, M., Stability of tetragonal ZrO<sub>2</sub> particles in ceramic matrices, *J. Am. Ceram. Soc.*, **65**(2), (1982) 642.
2. Lange, F. F., Transformation toughening Part 4; fabrication, fracture toughness and strength of Al<sub>2</sub>O<sub>3</sub>-ZrO<sub>2</sub> composites. *J. Mater. Sci.*, **17** (1982) 247.
3. Green, K. J., Critical microstructure for microcracking in Al<sub>2</sub>O<sub>3</sub>-ZrO<sub>2</sub> composites. *J. Am. Ceram. Soc.*, **65**(12) (1982) 610.
4. Ruehle, M., Claussen, N. & Heuer, A. H., Transformation and microcracking as complementary process in ZrO<sub>2</sub> toughened Al<sub>2</sub>O<sub>3</sub>. *ibid.*, **69**(3) (1986) 195.
5. Hori, S., Yoshimura, M. & Somiya, S., Strength-toughness relations in sintered and isostatically hot-pressed ZrO<sub>2</sub>-toughened Al<sub>2</sub>O<sub>3</sub> composites. *ibid.*, **69**(3) (1986) 169.
6. Masaki, T. & Shino, K., Mechanical behaviour of ZrO<sub>2</sub>-Y<sub>2</sub>O<sub>3</sub> Ceramics formed by hot-isostatic pressing. In *Advances in ceramics, science and technology of zirconia III*, eds S. Somiya, N. Yamamoto & H. Hanagida, The Am. Ceram. Soc. Inc., Columbus, OH. (1988), p. 709.
7. Tsukuma, K., Takahata, T. & Shiomi, M., Strength and fracture toughness of Y-TZP, Ce-TZP, Y-TZP/Al<sub>2</sub>O<sub>3</sub> and Ce-TZP/Al<sub>2</sub>O<sub>3</sub>. In *Advance in Ceramics Vol 24: science and technology of zirconia*, eds S. Somiya, N. Yamamoto & H. Hanagida, The Am. Ceram. Soc., Columbus, OH, (1988), p. 721.
8. Rajendran, R., Swain, M. V. & Rossell, H. J., Mechanical properties and microstructure of co-precipitation derived tetragonal Y<sub>2</sub>O<sub>3</sub>-ZrO<sub>2</sub>-Al<sub>2</sub>O<sub>3</sub> composites. *J. Mater. Sci.*, **23** (1988) 1805-12.
9. Shi, J. L., Li, B. S. & Yen, T. S., Mechanical properties of Al<sub>2</sub>O<sub>3</sub> particle-Y-TZP matrix composite and its toughening mechanism. *J. Mater. Sci.*, **28** (1993) 4019-22.
10. Tuan, W. H. & Brook, R. J., Sintering of heterogeneous composites. Part II: ZrO<sub>2</sub>-Al<sub>2</sub>O<sub>3</sub>. *ibid.*, **24** (1989) 1953.
11. Sudre, O. & Lange, F. F., Effect of inclusions on densifications. I: microstructural development in an Al<sub>2</sub>O<sub>3</sub> matrix containing a high volume fraction of ZrO<sub>2</sub> inclusions. *J. Am. Ceram. Soc.*, **75**(3) (1992) 519.
12. Tuan, W. H. & Brook, R. J., Sintering of heterogeneous ceramic composites. Part I: Al<sub>2</sub>O<sub>3</sub>-Al<sub>2</sub>O<sub>3</sub>. *J. Mater. Sci.*, **24** (1989) 1062.
13. Shi, J. L. & Yen, T. S., Densification and microstructure development of alumina/Y-TZP composite powder (Y-TZP-rich) compacts. *J. Europ. Ceram. Soc.*, **15** (1995) 363.
14. Shi, J. L., Ruan, M. L. & Yen, T. S., Processing of Nano-Y-TZP/Al<sub>2</sub>O<sub>3</sub> Composites. I: preparation and characterization of nano-Y-TZP/Al<sub>2</sub>O<sub>3</sub> composite powders. *J. Europ. Ceram. Soc.*, **15** (1995).